JOURNAL OF FORENSIC SCIENCES

J Forensic Sci, March 2010, Vol. 55, No. 2
doi: 10.1111/j.1556-4029.2009.01276.x
Available online at: interscience.wiley.com

PAPER

CRIMINALISTICS

Wei Chu,[1,2] *Ph.D.; John Song,*[1] *M.S.; Theodore Vorburger,*[1] *Ph.D.; James Yen,*[1] *Ph.D.; Susan Ballou,*[1] *M.S.; and Benjamin Bachrach,*[3] *Ph.D.*

Pilot Study of Automated Bullet Signature Identification Based on Topography Measurements and Correlations*†

ABSTRACT: A procedure for automated bullet signature identification is described based on topography measurements using confocal microscopy and correlation calculation. Automated search and retrieval systems are widely used for comparison of firearms evidence. In this study, 48 bullets fired from six different barrel manufacturers are classified into different groups based on the width class characteristic for each land engraved area of the bullets. Then the cross-correlation function is applied both for automatic selection of the effective correlation area, and for the extraction of a 2D bullet profile signature. Based on the cross-correlation maximum values, a list of top ranking candidates against a ballistics signature database of bullets fired from the same model firearm is developed. The correlation results show a 9.3% higher accuracy rate compared with a currently used commercial system based on optical reflection. This suggests that correlation results can be improved using the sequence of methods described here.

KEYWORDS: forensic science, ballistics identification, class characteristics, individual characteristics, striation, cross-correlation function

Firearms often leave unique, reproducible toolmarks on the fired bullets and cartridge cases. The analysis and comparison of these marks play an important role in forensic analysis for crime investigation. Traditionally, comparisons of striations on fired bullets have been performed manually by toolmark examiners under a comparison microscope. This approach can be time consuming. From the early 1990s, automated search and retrieval systems for the comparison of firearms evidence have been developed and used with considerable success (1–3). Currently, the Integrated Ballistics Identification System (now known as IBIS Heritage) (4) is widely used in U.S. forensic laboratories. The IBIS Heritage consists of a data acquisition station (DAS) and a signature analysis station (SAS). The DAS acquires images obtained with a reflection optical microscope under controlled illumination conditions. The signatures processed from the acquired images are compared with a relevant database in the SAS. The contrast of these images depends on the surface topography (peaks and valleys) of the bullet or casing. However, the correspondence between the image contrast and the surface topography is not one-to-one and is affected by many factors, including: the intensity and direction of the light source, the variation in material properties over the surfaces, and shadowing and multiple light scattering during reflection. At the National Institute of Standards and Technology (NIST), a correlation approach based on topography measurements was developed for the signature measurement and inspection of the NIST standard bullets and casings (5–7). Other researchers have also reported studies of topography methods for ballistics identification (8–10) and the development of a commercial system (11). Several approaches for automating the comparison of striation marks are based on extracting an averaged surface profile along the striation direction. The main differences between these approaches lie in the specific procedures for generating the averaged profile (8,12,13), removing surface curvature and otherwise filtering the profile, and selecting the effective correlation area, that is, avoiding *bad areas* from being used for correlation purposes. By *bad areas* we mean areas of the bullet surface that do not contain useful, reproduced striations. For example, some areas of the bullet may not be sufficiently contacted by the barrel during firing or may contain toolmarks that are not caused by contact with the barrel. Conventionally, high quality image input is required for effective correlation results (14). Data located in bad areas must either be removed from consideration, usually by manual intervention, or be included in the correlation, thus likely causing a decreased correlation score. Although manual intervention is generally used to select the area of interest, this effort can be time consuming and is a subjective process.

In this paper, an automated procedure, developed under a commercially available MATLAB software environment (The MathWorks, Natick, MA), for bullet signature correlation based on topography measurement is described. In the following sections, we discuss our method to estimate land engraved area (LEA) width as a class characteristic, we describe the detailed procedures for automatic selection of effective correlation areas, normalization of LEA

[1]National Institute of Standards and Technology, Gaithersburg, MD 20899.
[2]Harbin Institute of Technology, Harbin 150001, China.
[3]Intelligent Automation Inc., Rockville, MD 20855.

*Certain commercial equipment, instruments, or materials are identified in this paper to specify adequately the experimental procedure. Such identification does not imply recommendation or endorsement by the National Institute of Standards and Technology, nor does it imply that the materials or equipment identified are necessarily the best available for the purpose.

†Funding provided by the National Institute of Justice (NIJ) through the Office of Law Enforcement Standards (OLES) at NIST.

Received 1 Oct. 2008; and in revised form 3 Feb. 2009; accepted 7 Feb. 2009.

twist angle, and for generation of the extracted average profile. Finally we discuss an experimental result using 48 bullets fired from 12 barrels comprised of six different brands.

Estimation of Class Characteristics

When bullets are fired from a firearm, topography features inside the barrel produce toolmarks on the bullet surfaces that form characteristic features. On the one hand, the class characteristics, usually associated with macro topography features, represent the common characteristics of a group of firearms manufactured from the same rifling design, manufacturer, and tooling process. In forensic science, class characteristics help in the classification of the type and manufacturer of a firearm. On the other hand, the individual characteristics, associated with the micro topography, represent the unique characteristics of the firearm barrel. These are unique for different barrels, even those manufactured from the same production line. In forensic science, individual characteristics are used for the ultimate identification of an individual firearm (9,15).

Class characteristics include the caliber of the barrel; the shape, number, and width of the lands; and the direction of the rifling twist of the barrel. By using the information from class characteristics, the time and effort to perform subsequent detailed correlations can be dramatically reduced. The accuracy of subsequent correlations and proposed identifications can also be improved. Features on the bullet of the general rifling characteristics (GRC) such as caliber, land number, and twist direction are readily identified, unless obscured by surface damage. The IBIS, for example, uses the GRC to filter the database before correlations are performed (1). If all the GRC are within tolerances, individual characteristics may be considered for classifying bullets fired from different barrels. In Bachrach's research (8), widths of the LEA and the groove impression are used to distinguish bullets with different class characteristics.

The width of the LEA is a quantifiable parameter and an appropriate classification tool for bullets. It is also not prone to being affected by other factors, such as bullet material and the fitting tolerance between the bullet and the barrel. Figure 1 shows a LEA profile measured by confocal microscopy and the position of the border points, which are the minima in the transition areas and are marked by two square dots. The abscissa difference between the border points is defined as the LEA width. The LEA width may be determined with a small enough statistical uncertainty that it is useful as a class characteristic. If the LEA width is calculated from measurements parallel to the base of the bullet, it should be multiplied by the cosine of the twist angle. The calculation of twist angle will be introduced in the next section. At this point in the description, we are neglecting the small difference between the abscissa difference and the arc length around the curved LEA surface.

To analyze the effect of the width of the LEA for bullet classification, a sample of bullets fired by a variety of firearms created by Intelligent Automation, Inc. (IAI, Rockville, MD) is used (16,17). Nine different barrel models of 9 mm firearms, most of them frequently used in crimes, were fired in that study. The brand names were Beretta, Ruger, Smith & Wesson, Taurus, Browning, HiPoint, SIG Sauer, Bryco, and Glock. For Beretta, Ruger, Taurus, HiPoint, SIG Sauer, and Bryco, the barrels were consecutively manufactured. Among the samples created by IAI, we selected bullets that had been fired from two barrels of each brand. The selection also consisted of two brands of bullets, Winchester and Remington, fired from each barrel and two bullets of each brand. Bullets fired through Glock barrels are excluded because of the nature of their polygonal rifling, which makes them challenging for image acquisition systems (17). Bullets fired through Smith & Wesson and HiPoint barrels are also excluded because the numbers of lands on those are different from the others, which have six lands per barrel.

Therefore, 2 bullets × 2 ammo brands × 2 barrels × 6 firearm brands for 48 bullets are used for the study. With six lands per barrel, 288 LEA widths are calculated from a typical profile in each topography image obtained with a confocal microscope. The distribution histograms of LEA widths are plotted in Fig. 2. The histogram of LEA widths for bullets fired through the Bryco barrels is not plotted because there are almost no measurable transition areas between the land and the groove from which a width can be calculated. But this property may be considered as a class characteristic that distinguishes it from other barrel manufactures used in this study. Except for a slight overlap between bullets fired through Beretta and Ruger, the other distributions are separated from each other. If the widths of all six LEAs of each bullet are averaged, a distinct gap will be evident between the distributions of LEA

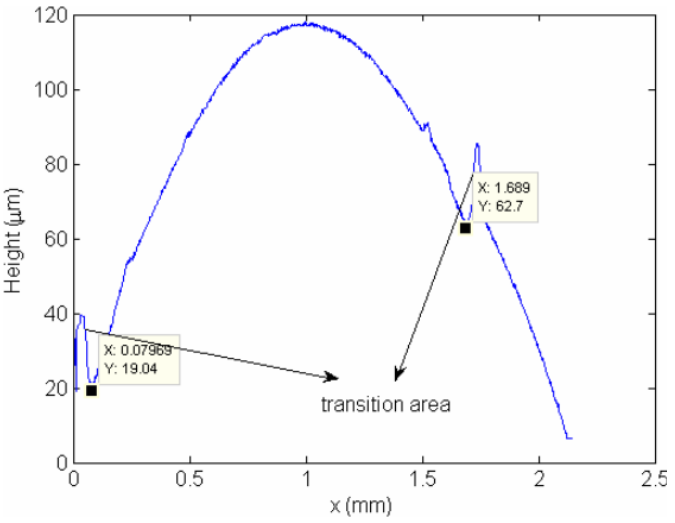

FIG. 1—*Calculation of LEA width.*

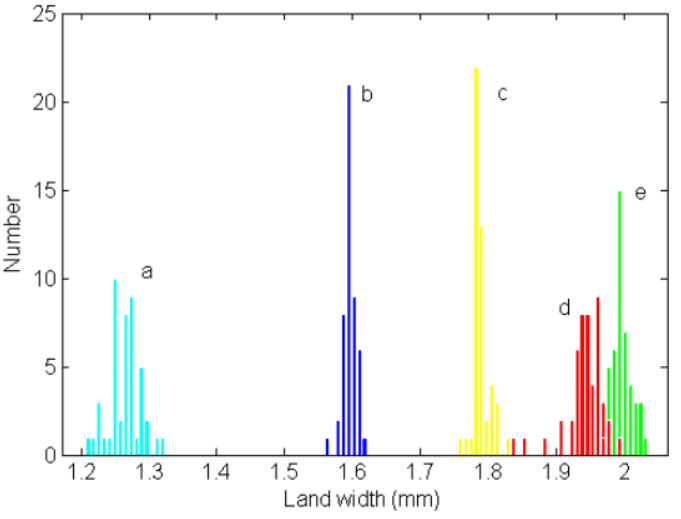

FIG. 2—*Histogram distributions of LEA widths for firearms of different manufacture. There are 48 entries for each type. Codes a, b, c, d, and e stand for Taurus, SIG Sauer, Browning, Beretta, and Ruger, respectively.*

widths for bullets fired through Beretta and Ruger barrels. Therefore, these brands can be distinguished by LEA width as well.

Automatic Calculation of Twist Angle and Selection of the Effective Correlation Area

Ideally, when a bullet is fired down the barrel, the rifling impression at every cross-section perpendicular to the axis of the bullet should be highly similar. The difference is a small shift between any two cross-sections caused by the twist of the barrel rifling that causes the bullet to spin. The twist angle is an important feature of the topography of the fired bullet. To calculate the twist angle, the cross-correlation technique, which has been used in firearms identification research as a metric for assessing similarity for both bullets and casings (5), is also used here to calculate the shift and the twist angle.

Figure 3 illustrates the selection of an effective correlation area and the calculation of the twist angle. The raw data are obtained from a bullet fired through a Beretta barrel, and imaged by the confocal microscope. After the truncation of data points outside the LEA, special processing is implemented (i) to remove dropouts and outlier data resulting from the limitations of the confocal microscope and (ii) to make interpolations over the resulting gaps in the data (16). Then a profile Gaussian filter (18) with 0.25 mm long-wavelength cutoff λ_c and 0.0078 mm short-wavelength cutoff λ_s is used to remove the low frequency waviness and high frequency noise. We use a Gaussian filter along horizontal profiles line by line instead of using an areal filter because the measured bullet impression topography consists essentially of profiles. These profiles have highly similar shape at different sections but a small shift between each section. After these processes, the flattened image is shown in Fig. 3*a*.

We next calculate the twist angle from the data. Suppose the total number of transverse profiles in this image is n. We take the first profile as the initial reference (the reference may change during the processing, as described below), and the remaining $n - 1$ profiles are correlated with the reference profile by the cross-correlation function (CCF). The CCF of two digitized profiles is given by:

$$\mathrm{CCF}(r, l_i, \tau) = \frac{\sum_k \left((r(k) - \overline{r})^{\times} (l_i(k+\tau) - \overline{l_i})\right)}{\sqrt{\sum_k (r(k) - \overline{r})^2} \sqrt{\sum_k (l_i(k+\tau) - \overline{l_i})^2}}, \quad (1)$$

where r represents the reference profile; l_i ($i = 1,2, \ldots, n-1$) represents one of the correlated profiles; $\overline{r}$ and $\overline{l_i}$ are the mean value of r and l_i; and $r(k)$ and $l_i(k)$ are values of the kth points on r and l_i. The location of the maximum of the correlation function, CCF_{max} (r, l_i,τ), indicates the shift τ_i leading to the best possible correlation between the two correlated profiles. To avoid nonsensical CCF calculations resulting from imperfect image quality or other factors, a threshold is set to limit the possible shift difference τ_i to a certain range. Depending on the twist direction, the allowable pixel shift between adjacent profiles l_{i+1} and l_i, is constrained, for example, to be (0, 1, 2) for a left-handed twist or (0, −1, −2) for a right-handed twist. The software contains a branch point where the reference profile is discarded and the next profile becomes the reference profile if the shift difference with respect to the previous profile is outside the above limits. The reason for this constraint is as follows. Generally, the twist angle is small and there is only a small change between adjacent transverse sections of a bullet in a good signature area. It is therefore concluded that the correlation information between two profiles is not correct if the shift τ_{i+1} has an abrupt change.

We plot in Fig. 3*b* all profile shifts τ_i with respect to the first profile calculated for Fig. 3*a*. This curve consists of a series of steps. The tilt angle of this curve is approximately equal to the

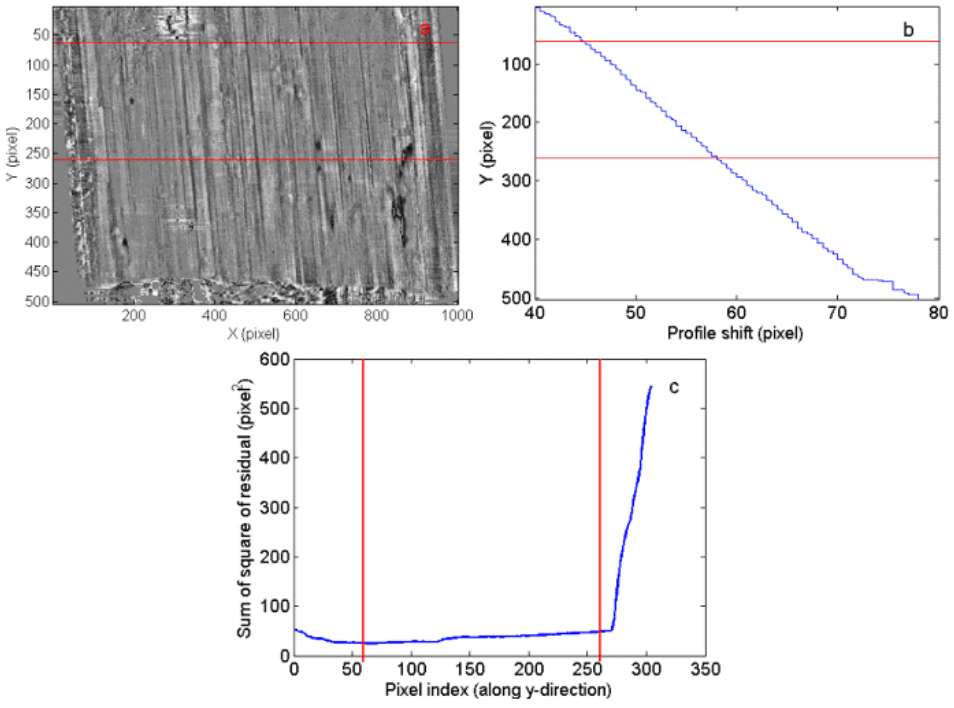

FIG. 3—*Selection of effective correlation area: (a) image after groove area truncation, dropout removal, interpolation, and band pass filter; (b) profile shift (abscissa) versus pixel index along the* y*-direction (ordinate); (c) sum of squares of residuals versus pixel index along the* y*-direction. The straight lines indicate the 200 profiles subarea calculated to be optimum for profile averaging and correlation.*

twist angle of the bullet image in Fig. 3*a*. Their different appearances are due to the different *x*-scales between the two figures. The angle can be obtained from the slope of the least squares fit of the curve.

An automatic selection of the effective correlation area is now performed whose generated average profile will represent the bullet signature where the striations are significant, that is, not worn flat or damaged. Using the algorithm described below, an area is selected consisting of 200 horizontal profiles (about 0.31 mm wide) to generate the extracted average profile instead of the whole image. The number 200 is specified because it is possible for most bullets used in the experiment to find an area with such a width that contains significant striation marks. Naturally, the more a correlation area contains significant striation marks and valid information, the more its step curve (Fig. 3*b*) will be consistent and straight. So a window with a height of 200 pixels (or 0.31 mm) is superimposed on the step curve. This window is moved vertically as part of a search for the most consistent and straight segment of the step curve, as shown in Fig. 3*b*. At each pixel position, a least squares fitting of data inside this window is performed, and its corresponding residual sum of squares (RSS) is calculated. The RSS is the sum of squares of residuals between a segment of the step curve and its corresponding fitting line. It is calculated by

$$\mathrm{RSS} = \sum_i^n (y_\mathrm{i} - f(x_\mathrm{i}))^2, \qquad (2)$$

where y_i is the fitting line and $f(x_\mathrm{i})$ the segment of the step curve. The most effective correlation area will be determined when the RSS reaches its minimum. For this example, the results are plotted in Fig. 3*c*. Note that the area spanning lines $y = 1$ to $y = 200$ has a pixel index equal to 1 in Fig. 3*c*. As can be seen in Fig. 3*c*, the minimum sum of squares of residual occurs at pixel position 60. Therefore, the area between the 60th and 259th row, with the best slope consistency in the image, is selected. In Fig. 3*a*, *b*, and *c*, the pair of straight borderlines represents the subarea used for determining the final twist angle and for generating the extracted average profile. Figure 4*a* shows the rotated image of the selected area. Then the extracted average profile (Fig. 4*b*) is generated by averaging all the columns of the rotated image. During the generation of the averaged profile, if a point whose difference with respect to the mean value of the whole 200-line image exceeds three times the standard deviation of the image, it is omitted as a noisy outlier data point. This is done to further reduce inclusion of erroneous information in the individual topography characteristics.

If a reasonable twist angle range is specified, this processing method is especially helpful when the significant striations are formed on only a portion of the bullet surface. Figure 5 gives such an example where areas that contain either incorrect striation information or no striations are automatically excluded by the above procedure. Figure 5*a* shows a flattened image, which has different striation patterns in the top, middle, and bottom portions. In the top area, the angles of the striations are less than the normal twist angle of the barrel. This is because these striations are formed in the early stage of the firing when the bullet has not fully engaged with the barrel. Such striations are termed *axial engravings*. Therefore, this area is automatically excluded from the start because of the steep slope of the step curve (see Fig. 5*b*), irrespective of the result of the sum of square of residual calculated subsequently from it. In Fig. 5*c*, this is the left (void) area of the dotted vertical line. Then the effective and informative correlation area is automatically selected from the remaining area.

Results

Once the average profile is determined for each LEA image, the cross-correlation values are computed between the LEAs of two bullets at all possible phases. A *phase* is a pairwise comparison of two bullets. In this experiment, each bullet has six LEAs, so two bullets are correlated at six possible phases. Figure 6 shows two such possible phases, where A1–A6 and B1–B6 stand for their six LEAs in order. Each LEA of A is correlated with each LEA of B, resulting in a 6 by 6 matrix with 36 cross-correlation values. If bullets A and B were fired through the same firearm, there would be one phase orientation where each LEA of A should be highly correlated with each LEA of B in succession. Accordingly, the customary correlation metric, called the "max phase" (1), is calculated here as the sum of the cross-correlation scores for six LEAs at the optimum phase orientation where that sum score is highest.

A program has been developed, which automates the methods discussed in the section Automatic Calculation of Twist Angle and Selection of the Effective Correlation Area, and produces cross-correlation scores at the "max phase" condition for each pair of bullets. Table 1 shows a combined list of averaged CCF values (one-sixth of the "max phase" cross-correlation score) for all eight bullets fired from the Ruger barrel. Indices 1–4 and 5–8 represent bullets fired from two different barrels. Note that none of the CCF values for nonmatching pairs is larger than any of the CCF values for matching pairs. Ranking lists are then developed for each bullet according to these "max phase" scores of correlation with the other seven bullets in the same type-of-firearm group. For each of these 48 ranking lists, the three other bullets fired from the same identical firearm should have the highest correlation scores and should occupy the top three positions in the list.

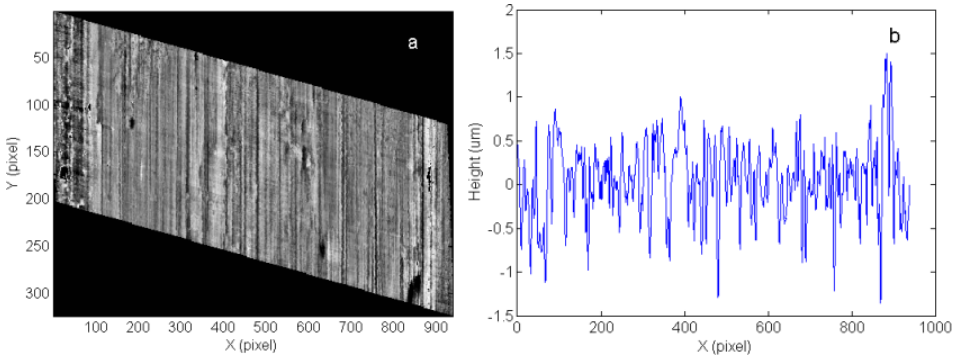

FIG. 4—*Generation of the extracted average profile: (a) rotated image in the effective correlation area and (b) generated averaged profile.*

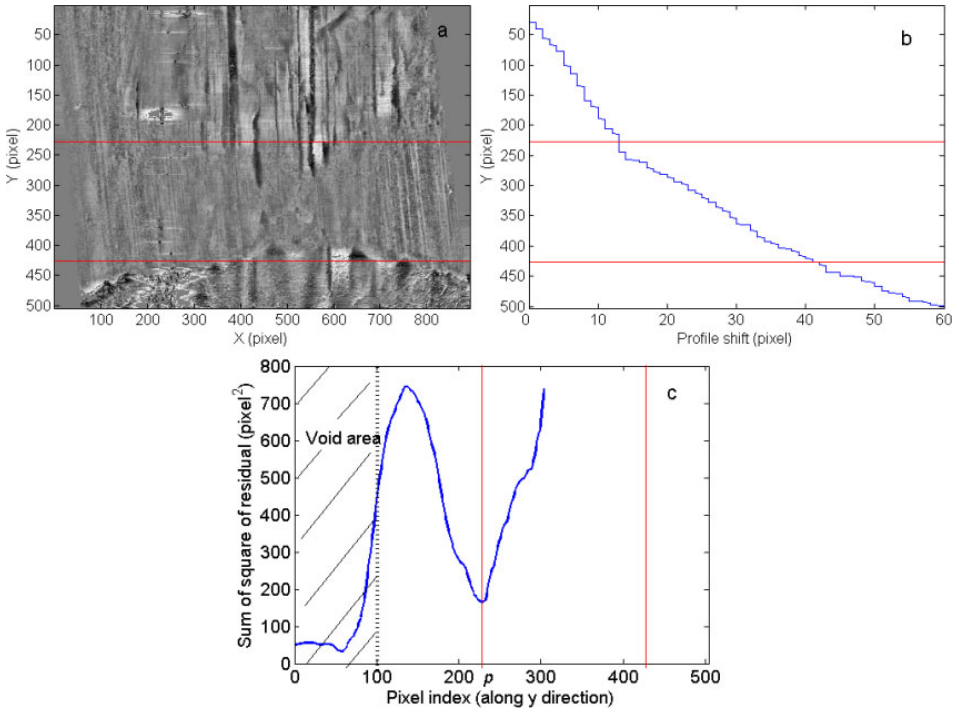

FIG. 5—*Bullet surface that partly contains effective striation marks: (a) flattened image, (b) step curve of the profile shift, and (c) sum of squares of residuals.*

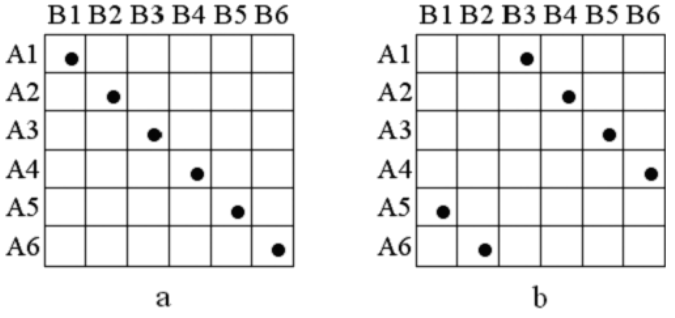

FIG. 6—*Examples of comparisons of bullet A (LEAs A1–A6) and bullet B (LEAs B1–B6) at two different phases: (a) A1 versus B1, A2 versus B2…A6 versus B6; (b) A1 versus B3, A2 versus B4…A6 versus B2.*

TABLE 1—*Averaged cross-correlation scores, calculated at the max phase position, for the eight bullets fired from Ruger barrels.*

Matching		Nonmatching			
Bullets Being Correlated	Average CCF for 6 LEAs	Bullets Being Correlated	Average CCF for 6 LEAs	Bullets Being Correlated	Average CCF for 6 LEAs
1 vs. 2	0.593	1 vs. 5	0.250	3 vs. 5	0.245
1 vs. 3	0.528	1 vs. 6	0.250	3 vs. 6	0.266
1 vs. 4	0.501	1 vs. 7	0.255	3 vs. 7	0.258
2 vs. 3	0.467	1 vs. 8	0.236	3 vs. 8	0.244
2 vs. 4	0.447	2 vs. 5	0.232	4 vs. 5	0.261
3 vs. 4	0.533	2 vs. 6	0.246	4 vs. 6	0.266
5 vs. 6	0.392	2 vs. 7	0.244	4 vs. 7	0.264
5 vs. 7	0.312	2 vs. 8	0.239	4 vs. 8	0.237
5 vs. 8	0.332				
6 vs. 7	0.517				
6 vs. 8	0.496				
7 vs. 8	0.582				

CCF, cross-correlation function; LEA, land engraved area.

For all 48 lists, the average number of correct matching bullets has a value of 2.13, where 3.0 would be a perfect score. This matching rate is about 9.3% higher than that obtained with a widely used commercial system where the images are acquired with optical microscopy (16). For the same database of 48 bullets, the average number of correct matching bullets is 1.85. Conversely, the error rate is about 24% smaller for the procedure described here.

Although several steps are automated under the procedure described here, manual operation is indispensable during the data acquisition, and manual intervention can also be introduced during the analysis. In case an unsatisfactory result occurs in any processing step, the operator can make a decision to accept the result or not. If not, the operator can redo and/or add operations manually, or re-enter the values of the input parameters for correlations. The average score of matching bullets discussed above can be improved further by manually removing dropouts and outliers and bad areas and by selecting the effective correlation area. Manual intervention currently provides significant beneficial effects for ballistics correlations, but the results strongly depend on the experience and skill of the operator.

We now introduce another output metric to characterize the quality of matches between multiple LEAs on bullets. When a LEA of bullet A is correlated with all the LEAs of B, we call the maximal correlation score the *LEA correlation peak* for that LEA. There is a different LEA correlation peak for each LEA of bullet A. However, if the match between the bullets is perfect, all the LEA correlation peaks should occur at a single phase between the bullets. Counting the number of LEA correlation peaks in each of six possible phases, there should be a clear maximum at the matching phase position, and that maximum is defined here as the *matching LEA index*. This quantity can be used to indicate the reliability of identifying bullets fired from the same firearm. The resulting integer ranges from 1 to 6. In the ideal situation of two bullets fired through the same firearm, the value should be 6 as suggested in Fig. 6. That is, all six LEAs should match the best when the phase

of the two bullets is optimized. By comparison, for a completely stochastic condition, the probabilities that the matching LEA number equals 6, 5, 4, 3, 2, and 1 denoted as N_6, N_5, N_4, N_3, N_2, and N_1, are

$$N_6 = \frac{C_6^1}{6^6} = 0.00013$$

$$N_5 = \frac{C_6^1 C_6^5 C_5^1}{6^6} = 0.00386$$

$$N_4 = \frac{C_6^1 C_6^4 C_5^1 C_5^1}{6^6} = 0.04823$$

$$N_3 = \frac{C_6^2 C_6^3 + C_6^1 C_6^3 \cdot \left(C_5^1 C_1^1 C_4^1 + C_5^1 C_4^1 C_5^1\right)}{6^6} = 0.3151$$

$$N_2 = \frac{C_6^3 C_6^2 C_4^2 + C_6^2 C_6^2 C_4^2 C_4^1 C_3^1 + C_6^1 C_6^2 C_5^1 C_4^1 C_3^1 C_2^1 C_1^1}{6^6} = 0.6173$$

$$N_1 = \frac{C_6^1 C_5^1 C_4^1 C_3^1 C_2^1 C_1^1}{6^6} = 0.0154$$

Here C_n^r stands for the number of ways of choosing r elements out of total n elements without repeating (19). As an example, the calculation of N_3 is described. The numerator includes two sum items. The first item, $C_6^2 C_6^3$, calculates the number of ways that all six LEA correlation peaks can be divided into two groups of three, located on two different phase diagonals. The second item calculates the number of ways that three LEA correlation peaks can be on one phase diagonal and the other three LEA correlation peaks are on other phase diagonals but *not* all on the same one. This item has two subitems depending on whether the first and second remaining peaks are on the same diagonal or not. Similarly, the numerator of N_2 includes three sum items. The first item calculates the number of ways that all six peaks are divided into three group of two and located on three different diagonals; the second item calculates the ways that two peaks are on one diagonal, two other peaks can be on another one but the remaining two peaks cannot be on one diagonal; and the third item calculates the ways that only two peaks are on one diagonal and no two of other four peaks can be on one diagonal. Note that $\sum_{i=1}^{6} N_i$ is equal to unity. The mathematical expectation, i.e., probability-weighted sum of the possible values, of the matching LEA index for a stochastic condition is equal to

$$6N_6 + 5N_5 + 4N_4 + 3N_3 + 2N_2 + N_1 = 2.4$$

The matching LEA index introduced here should have a close relationship to the image quality and reliability of a matching result. If correlated images have good quality and faithfully reflect the characteristic features of bullets, the matching bullets would most likely occupy the top position of the ranking list, and the matching LEA index would tend to have a higher value. By contrast, if the matching LEA index shows a low value, such as 3 or 2, it implies that the matching result may be just a stochastic result. For eight bullets, four fired from each of two barrels of the same brand, each bullet will have three matching pairs of bullets fired through the same barrel and four nonmatching pairs of bullets fired through the other barrel. The total number of pairs is 56, of which 24 are matching and 32 are nonmatching. The distribution of matching LEA indices for bullets fired through Ruger barrels are listed in Table 2. Among the 24 matching pairs, 18 pairs have a matching LEA index greater than or equal to 4. The remaining six pairs have a value equal to 3; all of them are related to bullet number 5. Moreover, the CCF value in Table 1 indicates that the image quality of bullet number 5 is not as good as other bullets fired through the same barrel brand. The bullets fired through the Beretta barrel yield a similar result because both of those sets of images yield data with strong characteristics. The matching LEA indices for the Taurus, Browning, SIG Sauer, and Bryco barrels are not as high as those of Beretta and Ruger barrels due to the relatively more stochastic quality of the acquired data. In Table 3, the number of correct matching bullets on the top three list and the average matching LEA index for all six brands are listed. There is a strong correlation between these two numbers, suggesting that the higher the matching LEA index is, the more reliable the matching result is.

An overlap metric p is also calculated here to characterize the quality of the separation (or the degree of overlap) between matching and nonmatching correlation score distributions. The overlap metric may be used for the probability distribution of any correlation parameter, but the specific parameter of interest here is the overlap metric for the probability distributions of matching and nonmatching CCF scores. The overlap metric describes the probability that the CCF value of a randomly chosen member of the nonmatching distribution is larger than the CCF value of a randomly chosen member from the matching distribution. As matching correlation scores should ideally be near 100% and nonmatching correlations should ideally be near zero, the probability that a nonmatching score exceeds a matching score should be at or near zero. If the two distributions were the same, then p would be 0.5. This overlap metric was used by Vorburger et al. (16) to characterize the separation of several different correlation data sets for breech face and firing pin impressions on casings, and similar parameters were developed earlier by Bachrach (17) to characterize the correlation data sets for fired bullets.

The overlap metrics are calculated here assuming that the different brands and models of firearms can be separated from one another using other parameter(s), such as LEA width described above. The overlap here would be considerably greater if one were not able to do this preliminary separation. The overlap metrics for bullets fired from the different brand barrels are listed in the fourth row of Table 3. These are determined by calculating the mean and standard deviation from the CCF data for matching and nonmatching pairs. The results become the parameters for Gaussian distributions describing the CCF data for the matching and nonmatching bullet pairs, respectively, for each brand. In this table, the identification of bullets fired from the Bryco barrels shows the most overlap. In fact, for the Bryco barrels used here, all three parameters in the table (number of correct matching bullets on top three list, average matching LEA index, and overlap metric p), are consistent with a completely random condition, where the scores would be 10.3, 2.4, and 0.5. By contrast, the computation for bullets fired from Ruger and

TABLE 2—*Distribution of matching LEA indices for Ruger barrels.*

	Matching LEA Index			
	6	5	4	Less than 4
Same barrel	8 pairs	8 pairs	2 pairs	6 pairs
Different barrel	0	0	0	32 pairs

LEA, land engraved area.

TABLE 3—*Correct matching bullet number and average matching LEA index for all brands.*

	Taurus	Bryco	Ruger	SIG	Browning	Beretta
Number of correct matching bullets on the top three list	14	9	24	16	15	24
Average matching LEA index number	2.63	2.25	4.75	2.45	2.63	4.75
Overlap metric p	0.277	0.554	0.006	0.217	0.271	0.026

LEA, land engraved area.

Beretta barrels gives high separation and low overlap metrics. A value of 0.006 in particular shows especially wide separation. This value would be consistent with an expected accuracy of about 90% if a true match is being sought in a top 10 list of correlations from a database of 1000 images. The overlap metric p calculated for Browning, Taurus, and SIG Sauer indicate a degree of randomness in the distributions, and reflect, to a certain extent, different challenges in bullet identification for different brands of barrels (see also Ref. [17] for additional discussion of this topic).

Summary and Future Work

It is well known that use of class characteristics effectively reduces the population of bullets that must be correlated using individual characteristics. Down-selection of bullets to be correlated reduces the database size and thereby improves the ranking of correct matches. We use LEA width as a class characteristic in this paper. Further, the procedure described here has the ability to automatically select the effective correlation area, calculate the twist angle, and extract an average profile, thus automatically filtering out, by class characteristics, information that is less resolving to individual characteristics, with the intent to produce higher correlation ratios for matching bullets.

Overall, we aim for methods that improve the accuracy of bullet correlations without significantly increasing the complexity of the processing. For this research so far, measuring six lands of a bullet with the confocal microscope takes about 15 min. Generating the correlation profile from an image depends on many factors, such as image size, image quality, and number of outliers. Typically, this processing may take 10–15 sec for the images we have described. Correlation time depends on the size of the database. It takes a fraction of a second for the tiny databases we use here, which only contain eight elements for each brand of firearm.

One important limitation of this study is the use of pristine bullets. Damaged bullets or fragments obtained at crime scenes present a much greater challenge for automated correlation and would require a more sophisticated procedure. In addition, the current version of the program can only distinguish the impression quality along the longitudinal (bullet axis) direction. It is not useful for the situation where informative areas are dispersed in both directions within the image. Further analysis should address this issue. In addition, the previous assumption that the areas to be correlated are rectangular can also be improved upon.

Acknowledgments

The authors are grateful to M. Ols of the Bureau of Alcohol, Tobacco, Firearms, and Explosives for IBIS acquisitions of bullets used in this study, to L. Ma of NIST for providing the software code used for dropout processing in the bullet image, and to R. Thompson and A. Hilton of NIST for helpful discussions.

References

1. Thompson RM. Automated firearms evidence comparison using the Integrated Ballistic Identification System (IBIS). In: Higgins K, editor. Investigation and forensic science technologies. Proceedings of SPIE, November 3, 1998, Boston, MA, SPIE, 1999;94–103.
2. http://www.forensictechnologyinc.com/DOWNLOADS/Publications/LargeDatabaseFinal.pdf (accessed November 25, 2008).
3. Braga AA, Pierce GL. Linking crime guns: the impact of ballistics imaging technology on the productivity of the Boston Police Department's Ballistics Unit. J Forensic Sci 2004;49(4):701–6.
4. http://www.forensictechnology.com/p7.html (accessed November 25, 2008).
5. Song J, Vorburger TV. Proposed bullet signature comparisons using autocorrelation functions. Proceedings of NCSL, July 16–20, 2000, Toronto, ON, Canada.
6. Song J, Whitenton E, Kelley D, Clary R, Ma L, Ballou S, et al. SRM 2460/2461 standard bullets and casings project. J Res Natl Stand Technol 2004;109(6):533–42.
7. Ma L, Song J, Whitenton E, Zheng A, Vorburger TV. NIST bullet signature measurement system for SRM (standard reference material) 2460 standard bullets. J Forensic Sci 2004;49(4):649–59.
8. Bachrach B. Development of a 3D-based automated firearms evidence comparison system. J Forensic Sci 2002;47(6):1253–64.
9. De Kinder J, Bonifanti M. Automated comparison of bullet striations based on 3D topography. Forensic Sci Int 1999;101(2):85–93.
10. Banno A, Masuda T, Ikeuchi K. Three-dimensional visualization and comparison of impressions on fired bullets. Forensic Sci Int 2004;3:233–40.
11. Dillon JH. BulletTRAX™-3D, MatchPoint Plus™ and the Firearms Examiner. Evidence Technology Magazine, July–August 2005.
12. Heizmann M. Automated comparison of striation marks with the system GE/2. In: Geradts ZJ, Rudin LI, editors. Investigative image processing II. Proceedings of SPIE, April 4, 2002, Orlando, FL, SPIE, 2002;80–91.
13. Puente León F. Automated comparison of firearm bullets. Forensic Sci Int 2006;156(1):40–50.
14. Puente León F, Beyerer J. Automatic comparison of striation information on firearm bullets. In: Casasent DP, editor. Intelligent robots and computer vision XVIII: algorithms, techniques, and active vision. Proceedings of SPIE, September 20–21 1999, Boston, MA, SPIE, 1999;266–77.
15. Song J, Rubert P, Zheng A, Vorburger TV. Topography measurements for determining the decay factors in surface replication. J Mea Sci Technol 2008;19(8):084005.
16. Vorburger T, Yen J, Bachrach B, Renegar TB, Filliben JJ, Ma L. Surface topography analysis for a feasibility assessment of a national ballistics imaging database. Gaithersburg, MD: National Institute of Standard and Technology, 2007 May. Report No.: NISTIR 7362.
17. Bachrach B. A statistical validation of the individuality of guns using 3D images of bullets. Washington, DC: Department of Justice, 2006 Mar. Report No.: 213674.
18. American Society of Mechanical Engineers. ASME B46.1-2002, Surface Texture, Surface Roughness, Waviness and Lay. New York, NY: American Society of Mechanical Engineers, 2003.
19. Bancroft TA, Han PH. Statistical theory and inference in research. New York, NY: M. Dekker, 1981.

Additional information and reprint requests:
Wei Chu, Ph.D.
Guest Researcher
National Institute of Standards and Technology
100 Bureau Drive, Stop 8212
Gaithersburg
MD 20899-8212
E-mail: wei.chu@nist.gov